IEEE Access
Multidisciplinary | Rapid Review | Open Access Journal

Received October 26, 2018, accepted November 12, 2018, date of publication November 23, 2018,
date of current version December 27, 2018.

Digital Object Identifier 10.1109/ACCESS.2018.2883219

Open-Circuit Fault Diagnosis of Neutral Point Clamped Three-Level Inverter Based on Sparse Representation

YUNJUN YU, (Member, IEEE), AND SHILEI PEI
School of Information Engineering, Nanchang University, Nanchang 330031, China

Corresponding author: Yunjun Yu (yuyunjun@ncu.edu.cn)

This work was supported in part by the National Natural Science Foundation of China under Grant 61563034 and in part by the Program of China International Science and Technology Cooperation Projects under Grant 2014DFG72240.

ABSTRACT Decomposition of the signal on the orthogonal or nonorthogonal basis of the signal space is the traditional method for fault feature extraction in the field of inverter fault diagnosis. These signal analysis methods make the result of signal decomposition not sparse and they are not self-adaptive. In recent years, sparse representation has received considerable attention in signal processing because the method can overcome the shortcomings of traditional methods by decomposing the signal on an over-complete dictionary instead of on an orthogonal or nonorthogonal basis. This paper proposes a combination of sparse representation and support vector machine (SVM) for the fault diagnosis of neutral point clamped (NPC) three-level inverter. First, the three-phase phase voltage signals are sampled as the characteristic signals for analysis. Then, the K-SVD algorithm is used as the fault feature extraction technology to obtain an over-complete dictionary and the sparse representation coefficients of the characteristic signals. The latter are used as the feature information for the characteristic signals. Finally, the SVM with powerful generalization capability is used as the fault identification method to identify NPC three-level inverter fault types according to the extracted feature information and analyze the fault diagnosis effect. Simulation experiments show that the combination of sparse representation and the SVM for fault diagnosis of NPC three-level inverters has the advantage of high diagnostic accuracy. The fault diagnosis method proposed in this paper is compared with other methods to further verify its superiority in the fault diagnosis of NPC three-level inverters.

INDEX TERMS Neutral point clamped three-level inverter, fault diagnosis, feature extraction, fault identification.

I. INTRODUCTION

In the field of distributed power generation (DG), inverter is the key device that converts DC signals into AC signals. Inverter can be divided into two groups: two-level inverter and multilevel inverter. Multilevel inverter can be sub-divided further into cascaded H-bridge (CHB) inverter, flying capacitor (FC) inverter, neutral point clamped (NPC) inverter [1]. The type of inverter studied in this paper is the NPC three-level inverter. Compared to a two-level inverter, the three-level inverter has the advantages of lower harmonic distortion in the voltage output, lower voltage stress in power switches, smaller capacity switches and higher working efficiency [2], [3]. For these reasons, it has received increasing attention from researchers. However, the three-level inverter consists of more power switches than two-level inverter, resulting in a more complex circuit structure and lower reliability. Therefore, the possibility of faults in three-level inverter is higher, and the types of faults are more diverse [4]. If the three-level inverter occurs faults, it will negatively affect the normal operation of the entire distributed power generation system [5]. It is very important to accurately locate and identify faults occurring in inverter, because the diagnosis results can provide a basis for appropriate personnel to repair, reducing the risks and economic losses caused by inverter faults [6].

For the fault diagnosis of NPC three-level inverter, two key problems need to be solved: the first is fault feature extraction, which means that a certain method is used to extract effective information about the different fault types (feature extraction technology is the precondition for fault diagnosis of the inverter); the second is fault identification, which means that a certain method is used to accurately

identify the fault types according to the extracted feature information [7], [8].

There have been several studies of fault feature extraction. The spectrum method for fault feature extraction is presented in [9] and [10], the essence of spectrum method is Fourier transform, which converts the signals from the time domain to the frequency domain to obtain the frequency domain information of the signals. However, the basis function of the Fourier transform is infinite, so this analysis method will lose all the time domain information of signals and does not have time resolution. Spectrum method is suitable for analyzing stationary signals whose frequency does not change over time, but its ability to analyze nonstationary signals is poor, giving it limitations in the field of fault diagnosis. The wavelet analysis method is proposed to extract the fault signals feature information in [11]–[14]. This method is a time-frequency analysis method, which can obtain both the time domain information and frequency domain information of the signals simultaneously. Thus this method can overcome the defect of the spectrum method which will loss the time domain information of analyzed signals. However, wavelet analysis is hampered by the difficulty in selecting the wavelet basis, and the method lacks adaptability. In [15], the method of empirical mode decomposition (EMD) is introduced into fault diagnosis to extract signals feature information. EMD is also a time-frequency analysis method that decomposes signals into a finite number of intrinsic mode functions (IMF). The method breaks the limit of the uncertainty principle, has good time-frequency focusing characteristics, and it can adaptively decompose signals into finite IMF components according to the characteristics of the signals itself. However, the method also have disadvantages, such as mode mixing and end effects, which can affect the accuracy of fault diagnosis. The principle component analysis (PCA) method for feature extraction of signals is proposed in [10] and [16]–[17]. This method is used to analyze the correlations between a large number of data and to reduce their dimensions. The data after dimension reduction are smaller but retain sufficient information of the original data. PCA not only makes data processing more convenient, but also avoids data redundancy. However, the method must assume that the data follow the Gaussian distribution and cannot directly deal with nonlinear or multimodal problems.

In terms of fault identification, many neural network methods have been studied. For example, The back propagation neural network (BPNN) identification method for fault diagnosis of inverter is proposed in [18]–[21]. BPNN has been widely used in pattern recognition and classification because of its strong learning ability and nonlinear approximation ability. However, BPNN suffers from problems such as slow convergence rate and local optimum.

In summary, the common fault feature extraction methods and fault identification methods can solve some problems, but have their own limitations. In order to improve the accuracy of inverter fault diagnosis, it is necessary to further improve from the two aspects of fault feature extraction and fault identification. A more effective fault feature extraction method needs to be proposed to accurately extract fault feature information that can represent the essential characteristics of the analyzed signals, and a more effective fault identification method needs to be proposed to accurately identify the different faults according to the extracted feature information.

Traditional signal analysis methods, such as Fourier transform, short-time Fourier transform, wavelet transform and wavelet packet transform, generally decompose signals on an orthogonal or nonorthogonal basis. In contrast, the method of sparse representation decomposes signals on an over-complete dictionary [22], [23]. The signals can be represented linearly by a small number of atoms that make up the over-complete dictionary [24]. Sparse representation can achieve a high degree of characterization and extraction of the internal structure and morphological details of signals. In addition, the method has the characteristics of flexibility and adaptability [22], [25]. Because sparse representation has many advantages, it is widely used in signal denoising, signal compression, feature extraction, and in other fields [25]. For example, In [26]–[28], sparse representation method is studied for fault feature extraction and the experimental results show that the method can extract effective fault feature information. In this paper, the K-SVD algorithm for sparse representation of signal is used to extract feature information of characteristic signals. This algorithm has two processes: sparse coding and dictionary update. Through this algorithm, an over-complete dictionary and a sparse representation coefficient matrix of characteristic signals can be obtained. Each column vector of the sparse representation coefficient matrix is considered as the eigenvector of the corresponding signal. The support vector machine (SVM) method is then used for fault identification in this paper. SVM has unique advantages in solving small-sample, nonlinear, and high-dimension problems [29], [30]. A fault diagnosis method based on PCA and SVM is proposed for three-phase rectifiers, and fault types have been accurately identified by SVM [31]. A new method based on FFT-RPCA-SVM is proposed for the cascaded H-bridge multilevel inverter, and the proposed method has high accuracy and efficiency compared to other fault diagnosis methods in [9].

The K-SVD and SVM will be used for fault diagnosis of NPC three-level inverter in this paper, where K-SVD is used for fault feature extraction and SVM is used for fault identification. The effectiveness of combining K-SVD and SVM will be verified by simulation experiments.

The remainder of this paper is divided into five parts: Section II analyzes the topology structure and fault types of the NPC three-level inverter; Section III analyzes the theory of the K-SVD algorithm in signal sparse representation; Section IV analyzes the theory of SVM; Section V carries on the simulation experiments to verify the rationality of the fault diagnosis method based on sparse representation and support vector machines; and Section VI summarizes the findings of this study.

II. NPC THREE-LEVEL INVERTER FAULT ANALYSIS

The circuit topology of NPC three-level inverter [3] is shown in Figure 1. The inverter consists of A, B, and C three-phase bridge arms. Taking A-phase bridge arm as an example, this consists of four power switches ($s_{a1} - s_{a4}$), four free-wheeling diodes ($VD_{11} - VD_{14}$), and two clamping diodes ($D_1 - D_2$). Each free-wheeling diode is connected in antiparallel with the power switch to provide a reverse conduction loop for the current. The clamp diode is used to connect the power switches and the midpoint of the DC side capacitor. The output three-phase phase voltage signals of the inverter are filtered by LC filter to supply power for the load. The three-phase bridge arms are composed of 12 power switches. The state of each power switch is controlled by the corresponding gate signal. When the gate signal is 1(high level), the power switch is turned on; when the gate signal is 0(low level), the power switch is turned off. The switching mode of the inverter is determined by the modulation strategy. Common modulation strategies include pulse width modulation (PWM), sinusoidal pulse width modulation (SPWM), and space vector pulse width modulation (SVPWM), etc. Among them, SVPWM modulation strategy has the advantages of small harmonic components and high DC utilization, therefore SVPWM modulation strategy is used to control the gate signals of the power switches in this paper.

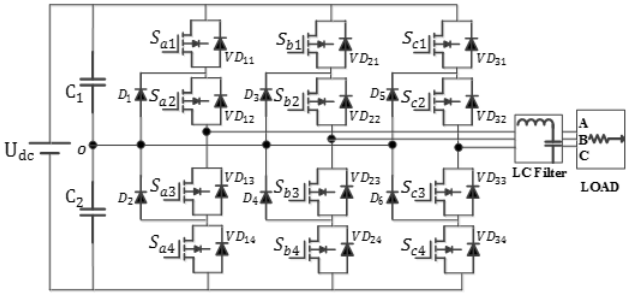

FIGURE 1. Circuit diagram of the NPC three-level inverter.

In the actual operation process, the NPC three-level inverter is prone to faults under high-frequency switching of power switches and complex environmental conditions. Most of the faults in the inverter are related to faults in the power switches, which include power switches open-circuit faults and short-circuit faults [32]. In general, short-circuit faults are avoided by the protection circuit. Once short-circuit faults occur in the power switches, the protection circuit is quickly disconnected, eventually converting the short-circuit faults into open-circuit faults [10]. Because short-circuit faults have a short time duration and are rapidly turned into open-circuit faults, this paper focuses on the diagnosis of open-circuit faults in NPC three-level inverter power switches only.

NPC three-level inverter power switches are consisted of 12 insulated-gate bipolar transistor (IGBT) devices. Due to the location and number of faulty power switches are random, there can be many types of open-circuit faults. In general, the possibility that three or more power switches all occur open-circuit faults at the same time is very small. This paper focuses on fault diagnosis in the case of open-circuit faults in one power switch or in two power switches. Open-circuit faults of power switches are divided into four categories: (1) the power switches all operating normally, which is considered a special fault condition; (2) only one power switch occurs open-circuit fault; (3) two power switches simultaneously occur open-circuit faults on a single-phase bridge arm; and (4) two power switches simultaneously occur open-circuit faults on two crossed arms. There are 73 fault types in these four fault categories, all of which will be discussed in this paper.

In normal operation, the three-phase phase voltage signals at the output of the NPC three-level inverter are sinusoidal, with a phase difference of 120°. If the power switches occur faults, the phase voltage signals at the output of the inverter will be changed. Different types of faults will generate different phase voltage signals, as shown in Figure 2. The three-phase phase voltage signals contain important information that reflects the characteristics of the faults. We can indirectly diagnose the faults by analyzing the three-phase phase voltage signals. In this paper, the three-phase phase voltage signals are used as the characteristic signals. The K-SVD algorithm is used to extract the fault feature information of three-phase phase voltage signals under different fault types, and the SVM method is used for fault identification to diagnose the faults in the inverter.

III. FEATURE EXTRACTION BASED ON SPARSE REPRESENTATION

A. BASIC IDEA OF SPARSE REPRESENTATION

Let $y_i \in R^m$ be a measured signal. $D = \left[d_1, d_2, \ldots, d_p\right] \in R^{m\times p}$ matrix is composed of a set of normalized vectors, we call D as a dictionary, and each vector d_i is an atom in dictionary D. If y_i can be represented linearly by a small number of atoms in D, there is a coefficient vector $x_i \in R^p$ such that $y_i \approx Dx_i$. The coefficient vector x_i is also called sparse code of the signal y_i.

$$(y_i) = \left(d_1, d_2, \ldots, d_p\right) \begin{pmatrix} x_i[1] \\ x_i[2] \\ \vdots \\ x_i[p] \end{pmatrix} \tag{1}$$

The objective function is:

$$\begin{aligned} &\min_{D,X} \|Y - DX\|_F^2 \\ &\text{subject to } \|x_i\|_0 \le S \quad \forall i = 1, 2, \cdots, n \end{aligned} \tag{2}$$

Where $Y = [y_1, y_2, \ldots, y_i, \ldots, y_n] \in R^{m\times n}$ is a series of signals to be analyzed, $D = \left[d_1, d_2, \ldots, d_p\right] \in R^{m\times p}$ is an over-complete dictionary, $X = [x_1, x_2, \ldots, x_i, \ldots, x_n] \in R^{p\times n}$ is a sparse representation coefficient matrix of Y, and S is the sparsity.

From the objective function, it can be shown that the sparse representation of signal is required to solve two problems, the learning of dictionary D and the solution of sparse

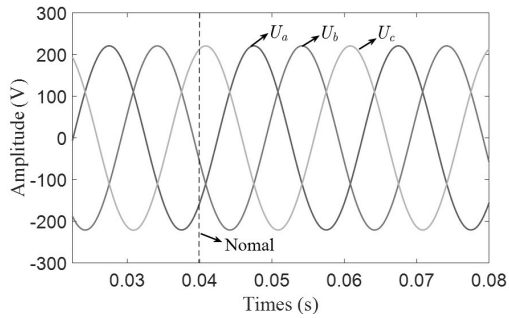

(a)

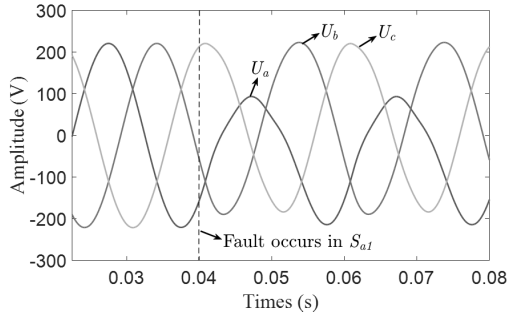

(b)

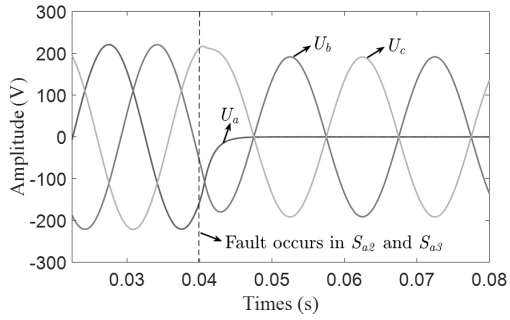

(c)

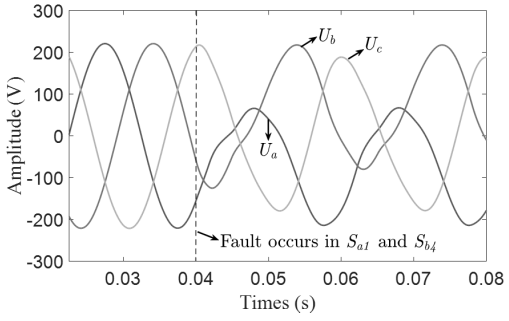

(d)

FIGURE 2. Phase voltage waveforms in different faults.

representation coefficient matrix X. Dictionary D and the sparse representation coefficient matrix X must satisfy two requirements: DX needs to approximate the original signals Y as much as possible, whereas the sparse representation coefficient matrix X needs to satisfy sparsity constraint. In this paper, the K-SVD algorithm is used to solve this problem.

B. K-SVD ALGORITHM

The K-SVD algorithm [33], [34] is an iterative algorithm which is an extension of the k-means algorithm, and is generally used to solve the dictionary learning problem in sparse representation of signal. Dictionary D in the K-SVD algorithm is an over-complete dictionary, and original signals can be approximate represented by a linear combination of atoms in D. The K-SVD algorithm essentially embodies the idea of data compression. The algorithm consists of two processes, as shown in Figure 3, namely sparse coding process and dictionary update process. The two processes are alternated until the requirements of the target equation are met.

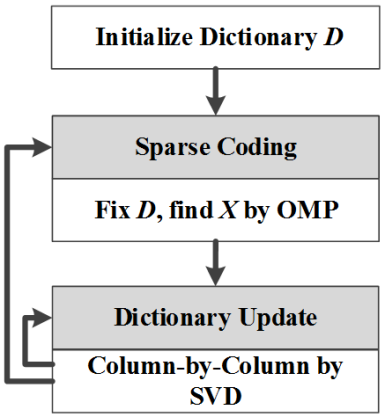

FIGURE 3. Flow chart of K-SVD algorithm.

1) SPARSE CODING PROCESS

The common algorithms of sparse coding include the base pursuit (BP) algorithm [35], [36], the matching pursuit (MP) algorithm [37], [38], and the orthogonal matching pursuit (OMP) algorithm [39], etc. In sparse representation of signal, the sparse coding problem is also to solve an optimization problem. We can write the following objective function:

$$\min_{X \in R^{p \times n}} \|Y - DX\|_F^2 \quad \text{subject to } \|x_i\|_0 \leq S \quad \forall i = 1, 2, \cdots, n \tag{3}$$

In the process of sparse coding, dictionary D is fixed, and our aim is to find the best sparse representation coefficient matrix X to represent original signals Y. The application of the OMP algorithm in the sparse coding process will be introduced as follows:

step 1. Initialize residual: r (*residual*) $\leftarrow y_i, x_i \leftarrow 0$.
step 2. $\Upsilon = \phi, t = 0$.
step 3. Select an atom that has the largest correlation with the residual:

$$\hat{l} \leftarrow \arg\max \left| d_i^T r \right|$$
$$i = 1, 2, \ldots, p$$
$$\Upsilon \leftarrow \Upsilon \cup \left\{ \hat{l} \right\}$$

step 4. Update residuals and coefficients:

$$r \leftarrow \left(I - D_\Upsilon \left(D_\Upsilon^T D_\Upsilon\right)^{-1} D_\Upsilon^T\right) r$$
$$x_i \begin{bmatrix} \wedge \\ l \end{bmatrix} \leftarrow x_i \begin{bmatrix} \wedge \\ l \end{bmatrix} + \left(\left(D_\Upsilon^T D_\Upsilon\right)^{-1} D_\Upsilon^T\right) r$$
$$t = t + 1$$

step 5. While $t \leq S$, repeat steps 3 and 4.
step 6. $y_i = Dx_i + r$.

We know that the residual obtained by the OMP algorithm is orthogonal to all the selected atoms. The atoms that have participated in the iteration will not participate in the subsequent iterations, that is, each atom only participates in one iteration. Thus the number of iterations will be reduced compared with the MP algorithm. The OMP algorithm will be used to obtain the sparse representation coefficient matrix of the signals instead of the MP algorithm.

In the sparse coding process of K-SVD algorithm, we can obtain the sparse representation coefficient matrix X of the signals Y on a given dictionary D.

2) DICTIONARY UPDATE PROCESS

In the K-SVD algorithm, the atoms of the dictionary are updated column by column, that is, only one column in dictionary D and the corresponding row in sparse representation coefficient matrix X are updated and the other columns in D and the corresponding rows in X are fixed at the same time. When a column is updated, the other columns are updated sequentially in the same way. After p iterations, a complete update of dictionary D is completed. The objective function is written as follows:

$$\begin{aligned} \|Y - DX\|^2 &= \left\| Y - \sum_{j=1}^{p} d_j g_j \right\|^2 \\ &= \left\| \left(Y - \sum_{j \neq k} d_j g_j \right) - d_k g_k \right\|^2 \\ &= \|E_k - d_k g_k\|^2 \end{aligned} \tag{4}$$

Where d_j is the jth column of dictionary D, g_j is the jth row of sparse representation coefficient matrix X, and E_k is the error after removing the kth atom. The purpose of the dictionary update is to find a new d_k and a new g_k to minimize $\|E_k - d_k g_k\|^2$. The SVD method can solve this problem. Decomposing E_k using SVD, we can get $E_k = U \Lambda V^T$, where U and V are unitary matrices, and Λ is a diagonal matrix with elements that are arranged in descending order. Take the first column vector of U as a new d_k, take the product of the first column vector of V and the first element of Λ as a new g_k. However, there is a problem with the above process. The desired sparse representation coefficient matrix is sparse, but the new g_k may make the sparse representation coefficient matrix unsparse. Therefore, the dictionary update process needs further processing as follows:

$$\|Y - DX\|^2 = \|E_k - d_k g_k\|^2 = \|E_k(J) - d_k g_k(J)\|^2 + c \tag{5}$$

Where $g_k(J)$ is the abbreviated matrix composed of nonzero elements in g_k, and $E_k(J)$ is the abbreviated matrix of E_k. The position of the g_k nonzero element determines the abbreviated matrix $E_k(J)$ of E_k. Decomposing matrix $E_k(J)$ by SVD, we can gain a new d_k and a new g_k. We can replace the previous d_k with the new d_k. Similarly, we can update other atoms.

In this paper, the K-SVD algorithm is used for feature extraction of signals, the four-step procedure for which is as follows:

step 1. Collect the characteristic signals (three-phase phase voltage signals) of different fault types as samples, and divide the samples into training samples and testing samples.
step 2. The K-SVD algorithm is used to obtain an over-complete dictionary D as well as the corresponding sparse representation coefficient matrix *X_train* according to training samples.
step 3. The OMP algorithm is used to obtain the sparse representation coefficient matrix *X_test* of the testing samples on the over-complete dictionary D.
step 4. *X_train* is regarded as the feature information of the training samples and *X_test* is regarded as the feature information of the testing samples.

The sparse representation coefficient matrix X is used as the feature information of the signals Y. In this way, we can complete the signals feature extraction task. Next we need to study fault identification method to identify the fault based on the extracted feature information.

IV. FAULT IDENTIFICATION BASED ON SUPPORT VECTOR MACHINE

After extracting the feature information of the signals, we need to accurately identify the fault types based on the extracted feature information. Thus a fault identification method is needed, which, for this paper, is SVM [40]. As a machine learning algorithm, it comes from statistical learning theory and structural risk minimization principles [30], [41]. SVM has been widely used in classification and regression problems due to its robustness and good generalization capabilities [42]. The basic idea of SVM for classification is to construct a hyperplane as the decision surface, which maximizes the separation distance between two classes of data samples [29], [41]. The following discussion will introduce the basic principles of two-class classification and multiclass classification problems.

A. TWO-CLASS CLASSIFICATION PROBLEM

Assume that there are two classes data samples (x_i, y_i), $x_i \in R^p$, $y_i \in \{+1, -1\}$, $i = 1, 2, \ldots, n$.

The optimal hyperplane problem is an optimization constraint problem, It can be achieved by solving the dual

problems as follows:

$$\max_{\alpha} \sum_{i=1}^{n} \alpha_i - \frac{1}{2} \sum_{i=1}^{n} \sum_{j=1}^{n} \alpha_i \alpha_j y_i y_j K\left(x_i, x_j\right)$$
$$\text{subject to } \sum_{i=1}^{n} \alpha_i y_i = 0, \quad C \geq \alpha_i \geq 0, \ i = 1, 2, \ldots, n \tag{6}$$

Where $C \geq 0$ is the penalty parameter of the error term, $K\left(x_i, x_j\right)$ is a polynomial kernel function that performs the non-linear mapping into the feature space. By solving (6), we can get the optimal solution $\alpha^* = \left[\alpha_1^*, \alpha_2^*, \ldots, \alpha_i^*, \ldots, \alpha_n^*\right]$. Each α_i^* in α^* is a nonzero vector, which is also called support vector.

Correspondingly, the optimal decision function is:

$$f(x) = \operatorname{sgn}\left[\sum_{i=1}^{n} \alpha_i^* y_i K\left(x_i, x\right) + b^*\right] \tag{7}$$

Where b^* is the classification threshold, select a positive component α_j^* of α^*, and b^* can be solved by the following equation:

$$b^* = y_j - \sum_{i=1}^{n} \alpha_i^* y_i K\left(x_i, x_j\right) \tag{8}$$

B. MULTICLASS CLASSIFICATION PROBLEM

SVM was originally designed to solve the two-class classification problem. When dealing with multiclass problems, it is necessary to construct a multiclass classifier [43]–[45]. Combining several binary classifiers to construct a multiclass classifier is a general approach to generalizing two-class SVM to multiclass SVM. One-against-all, one-against-one and directed acyclic graph SVM (DAGSVM) are common multiclass methods. In this paper, the one-against-one method is used for multiclass fault identification.

The one-against-one method is used to design an SVM between any two class samples, so K-class needs to design $K(K-1)/2$ subclassifier SVMs. When training class i and class j subclassifier SVM_ij, the ith sample is used as a positive sample and the jth sample is used as a negative sample. For the testing sample x, if the subclassifier SVM_ij considers it to be the ith class, the number of votes for the ith class is increased by one, if the subclassifier SVM_ij considers it to be the jth class, the number of votes for the jth class is increased by one. After voting by $K(K-1)/2$ subclassifiers, the testing sample belongs to the class with the most votes. One-against-one method is shown in Figure 4.

After constructing multiclass classifiers, the multiclass SVM can be used to identify fault types. The input of the SVM is the eigenvector, that is, the sparse coding of the original signal, and the output is the fault type label. First, the data sets are divided into training samples and testing samples. Then, training samples are used to train the SVM to obtain the training model. Finally, testing samples are predicted by the model, the predicted labels are compared with the actual labels to get the correct rate of fault diagnosis.

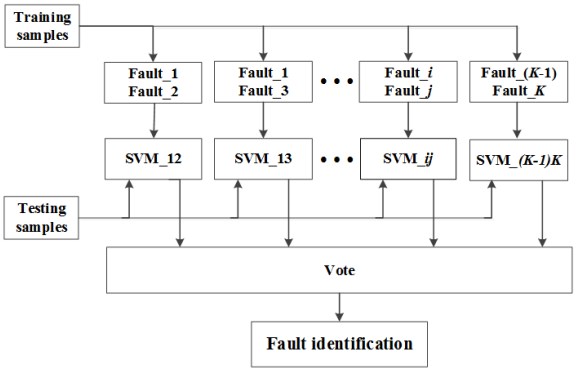

FIGURE 4. Structure diagram of one-against-one multiclass method.

The steps for fault diagnosis of NPC three-level inverter based on sparse representation and SVM are as follows: (1) build an NPC three-level inverter simulation model to simulate various fault types; (2) sample three-phase phase voltage signals. The phase voltage signals have periodicity, so each phase voltage signal is sampled ten times in one period and three-phase phase voltages therefore comprise 30 points, which constitute the characteristic signals to be analyzed; (3) the collected data are divided into training samples and testing samples, the training samples are processed by the K-SVD algorithm to obtain an over-complete dictionary D and sparse representation coefficient matrix X_train; (4) the sparse representation coefficient matrix X_test of the testing samples is obtained by the OMP algorithm; (5) train SVM with training samples to obtain a multiclass SVM model; (6) testing samples are used for prediction; and (7) compare the actual outputs and predicted outputs of the SVM to analyze the correct rate of fault diagnosis. The fault diagnosis flow chart shown in Figure 5.

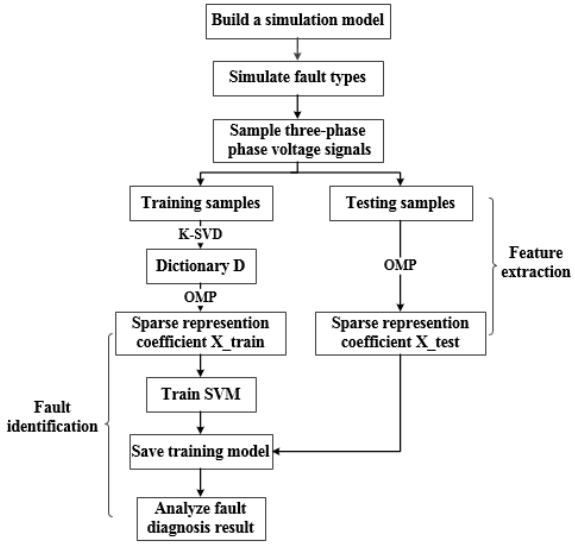

FIGURE 5. Flow chart of fault diagnosis.

TABLE 1. Encoding and labeling of the faults in NPC three-level inverter.

Fault Type	Code	Label	Fault Type	Code	Label	Fault Type	Code	Label
Nomal	000000000000	1	$S_{a1}S_{b4}$	000010000001	26	$S_{a1}S_{c3}$	010000000001	51
S_{a1}	000000000001	2	$S_{a1}S_{c4}$	100000000001	27	$S_{b1}S_{a3}$	000000010100	52
S_{a2}	000000000010	3	$S_{b1}S_{a4}$	000000011000	28	$S_{b1}S_{c3}$	010000010000	53
S_{a3}	000000000100	4	$S_{b1}S_{c4}$	100000010000	29	$S_{c1}S_{a3}$	000100000100	54
S_{a4}	000000001000	5	$S_{c1}S_{a4}$	000100001000	30	$S_{c1}S_{b3}$	000101000000	55
$S_{a1}S_{a3}$	000000000101	6	$S_{c1}S_{b4}$	000110000000	31	$S_{a2}S_{b4}$	000010000010	56
$S_{a2}S_{a3}$	000000000110	7	$S_{a1}S_{b1}$	000000010001	32	$S_{a2}S_{c4}$	100000000010	57
$S_{a1}S_{a4}$	000000001001	8	$S_{a1}S_{c1}$	000100000001	33	$S_{b2}S_{a4}$	000000101000	58
$S_{a2}S_{a4}$	000000001010	9	$S_{b1}S_{c1}$	000100010000	34	$S_{b2}S_{c4}$	100000100000	59
S_{b1}	000000010000	10	$S_{a4}S_{b4}$	000010001000	35	$S_{c2}S_{a4}$	001000001000	60
S_{b2}	000000100000	11	$S_{a4}S_{c4}$	100000001000	36	$S_{c2}S_{b4}$	001010000000	61
S_{b3}	000001000000	12	$S_{b4}S_{c4}$	100010000000	37	$S_{a1}S_{b2}$	000000100001	62
S_{b4}	000010000000	13	$S_{a2}S_{b3}$	000001000010	38	$S_{a1}S_{c2}$	001000000001	63
$S_{b1}S_{b3}$	000001010000	14	$S_{a2}S_{c3}$	010000000010	39	$S_{b1}S_{a2}$	000000010010	64
$S_{b2}S_{b3}$	000001100000	15	$S_{b2}S_{a3}$	000000100100	40	$S_{b1}S_{c2}$	001000010000	65
$S_{b1}S_{b4}$	000010010000	16	$S_{b2}S_{c3}$	010000100000	41	$S_{c1}S_{a2}$	000100000010	66
$S_{b2}S_{b4}$	000010100000	17	$S_{c2}S_{a3}$	001000000100	42	$S_{c1}S_{b2}$	000100100000	67
S_{c1}	000100000000	18	$S_{c2}S_{b3}$	001001000000	43	$S_{a3}S_{b4}$	000010000100	68
S_{c2}	001000000000	19	$S_{a2}S_{b2}$	000000100010	44	$S_{a3}S_{c4}$	100000000100	69
S_{c3}	010000000000	20	$S_{a2}S_{c2}$	001000000010	45	$S_{b3}S_{a4}$	000001001000	70
S_{c4}	100000000000	21	$S_{b2}S_{c2}$	001000100000	46	$S_{b3}S_{c4}$	100001000000	71
$S_{c1}S_{c3}$	010100000000	22	$S_{a3}S_{b3}$	000001000100	47	$S_{c3}S_{a4}$	010000001000	72
$S_{c2}S_{c3}$	011000000000	23	$S_{a3}S_{c3}$	010000000100	48	$S_{c3}S_{b4}$	010010000000	73
$S_{c1}S_{c4}$	100100000000	24	$S_{b3}S_{c3}$	010001000000	49			
$S_{c2}S_{c4}$	101000000000	25	$S_{a1}S_{b3}$	000001000001	50			

V. SIMULATION EXPERIMENT ANALYSIS

BPNN and SVM classifiers are used for fault identification in simulation experiments. Therefore, it is necessary to clarify the input and output of the two classifiers. According to the requirements of the comparison experiment, the input of the each classifier is the fault feature information extracted by different feature extraction methods, and the output corresponds to the fault types. When using BPNN for fault identification, the fault types are represented by the 12-bit binary code X12X11X10X9X8X7X6X5X4X3X2X1. The 12-bit binary code corresponds to 12 power switches, 0 means normal and 1 means fault has occurred. For example, 000000000000 indicates that the 12 power switches are normal, 000000000001 indicates that S_{a1} occurs open-circuit fault, and 001000010000 indicates that S_{b1} and S_{c2} both occur open-circuit faults. When using SVM for fault identification, the fault types are represented by the labels Label 1, Label 2, ..., Label 73, which correspond to the 73 types of fault. And the detailed representation is shown in Table 1.

A. INFLUENCE OF K-SVD ALGORITHM PARAMETERS SETTING ON RECONSTRUCTION ERROR

The K-SVD algorithm is used for fault feature extraction. The signals Y can adaptively learn a dictionary D and a sparse representation coefficient matrix X by the algorithm, and Y can be approximated by DX, which is $Y \approx DX$. We call $\|Y - DX\|_F^2$ the reconstruction error. This experiment will analyze the influence of the parameters of the K-SVD algorithm on the reconstruction error.

Taking into account the effects of temperature, light intensity,load, etc., the DC voltage at the inverter input and the load at the inverter output can be changed to obtain samples under different fault types. The three-phase phase voltage signals U_a, U_b, U_c are sampled under 450V/45kw, 450V/50kw, 450V/55kw, 500V/45kw, 500V/50kw, 500V/55kw. 550V/45kw, 550V/50kw, and 550V/55kw as samples. The total number of samples is 657. The phase voltage signals have periodicity, and each phase voltage is sampled ten times in one period, so three-phase phase voltages comprise 30 points, which constitute the characteristic signals to be analyzed. Finally, we get a 30×657 sample matrix, where 657 represents the number of samples and 30 represents each sample dimension. We use these samples to verify the influence of K-SVD algorithm different parameters on the reconstruction error. In Figure 6, (a) represents the reconstruction error at different iteration times, where the number of atoms is 40, the sparsity is 4, and the number of iteration times is 1–10; (b) represents the reconstruction error at different dictionary atom numbers, where the sparsity is 4 and the number of atoms is 45–60; (c) represents the reconstruction error at different values of sparsity, where the number of atoms is 40 and the sparsity is 2–7. Experiment results show that the number of iterations, the number of atoms in the dictionary, and the sparsity all affect the reconstruction error of the signals. In addition, the reconstruction error $\|Y - DX\|_F^2$ is related to the sparse representation coefficient matrix X, that is, different parameters will result in different sparse representation coefficient matrix X. Each column vector of sparse representation coefficient matrix X is considered as the eigenvector of the corresponding signal, and the eigenvector is the basis of fault diagnosis, thus the parameter setting will eventually affect the accuracy of fault diagnosis.

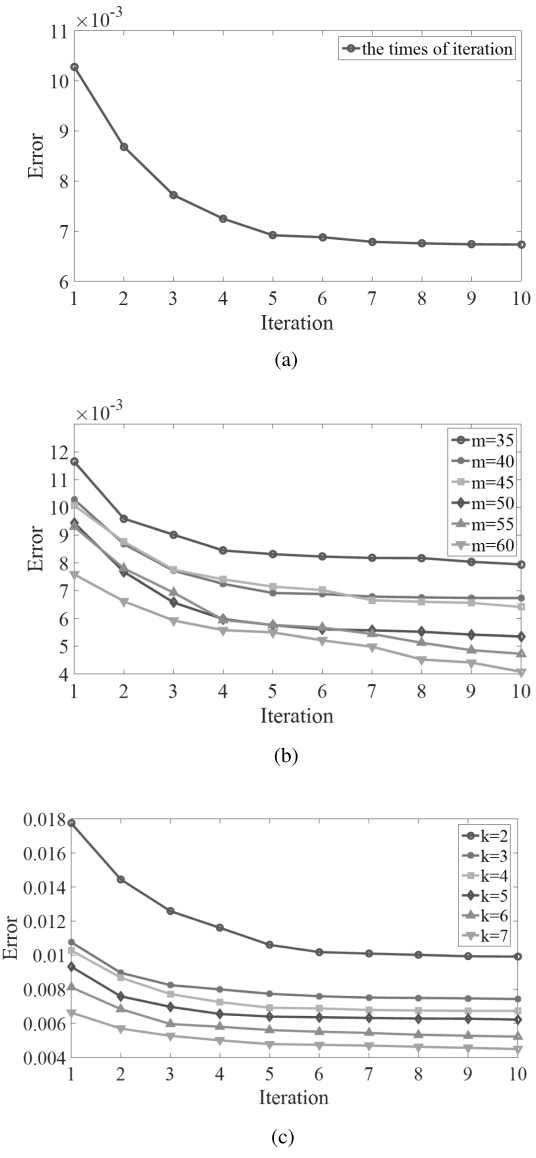

FIGURE 6. Reconstruction errors for different parameters.

B. COMBINATION OF SPARSE REPRESENTATION AND SUPPORT VECTOR MACHINE

This experiment is used to verify the effect of the combination of sparse representation of signal and SVM for NPC three-level inverter fault diagnosis. The 657 data samples sampled in Experiment A are used as training samples. The three-phase phase voltage signals U_a, U_b, U_c are sampled under 520V45kw, 520V50kw and 520V55kw as testing samples. The total number of testing samples is 219, making up a 30×219 testing sample matrix. From Experiment A, it can be seen that different parameters of the K-SVD algorithm will result in different sparse representation coefficient matrix X, and coefficient matrix X is used as the fault feature of the characteristic signals, which has a direct impact on the effect of fault diagnosis. Therefore, the parameters setting will eventually affect the accuracy of fault diagnosis.

In this experiment, the number of iterations is set to 10, the number of dictionary atoms is set to 40, and sparsity is set to 4, which means that the maximum number of nonzero elements in the each column vector of sparse coefficient matrix X is 4. In Table 2, (6,1) 0.04657, (15,1) 0.42777, (30,1) 0.11003, (35,1) 0.09975 means that the 6th, 15th, 30th, and 35th atoms, respectively, in dictionary D are activated and the other atoms are not activated. The signal can be represented linearly by these four atoms, and the representation coefficients are 0.04657, 0.42777, 0.11003, 0.09975, respectively. The vector $[0, \cdots, 0.04657, \cdots, 0.42777, \cdots, 0.11003, \cdots, 0.09975, \cdots 0]$ is a eigenvector of the corresponding signal. Because the number of dictionary atoms is 40, the sparse code of the signal consists of 40 elements, the number of nonzero elements is 4, and the remaining 36 elements are all 0. We can use the K-SVD algorithm to get the sparse representation coefficient matrix X of the training samples and testing samples. Then, the SVM method is used for fault identification. Figure 7 shows the identification result of the testing samples. Compared with the actual label and the predicted label of the testing samples, only one sample was misdiagnosed, the accuracy of fault diagnosis of the testing sample reaches 99.54%. The simulation experiment shows that the method used in this paper has the advantage of high diagnostic accuracy and can be successfully used for the fault diagnosis of NPC three-level inverter.

TABLE 2. Sparse results for different faults.

Label	Sparse Result			
1	(6,1)	(15,1)	(30,1)	(35,1)
	0.04657	0.42777	0.11003	0.09975
2	(21,2)	(28,2)	(29,2)	(31,2)
	0.07687	0.05568	0.47018	0.12299
3	(10,3)	(19,3)	(28,3)	(29,3)
	0.03125	0.03316	0.066198	0.67799
4	(1,4)	(3,4)	(16,4)	(35,4)
	0.63905	0.04199	0.02418	0.03748
5	(3,5)	(5,5)	(21,5)	(40,5)
	0.01926	0.05021	0.07938	0.67338
6	(1,6)	(8,6)	(16,6)	(35,6)
	0.79923	0.06949	0.05125	−0.14968
7	(3,7)	(5,7)	(13,7)	(21,7)
	0.030363	0.01692	0.61330	−0.01072
8	(15,8)	(21,8)	(32,8)	(35,8)
	0.88045	−0.17857	−0.097	−0.08222
9	(1,9)	(16,9)	(28,9)	(36,9)
	−0.01263	0.72978	0.03395	−0.03797
10	(12,10)	(20,10)	(25,10)	(32,10)
	−0.17761	0.59313	0.23269	0.05825
11	(5,11)	(12,11)	(24,11)	(32,11)
	0.18848	−0.0957	0.59451	0.05293
12	(10,12)	(17,12)	(21,12)	(28,12)
	0.06619	0.73851	−0.02805	−0.0816

C. COMPARISON EXPERIMENT OF DIFFERENT METHODS

To further confirm the superiority of the combination of sparse representation of signal and the SVM method, four groups comparison experiments are carried out in this experiment, including wavelet packet transform-BPNN, wavelet packet transform-PCA-BPNN, sparse representation-BPNN,

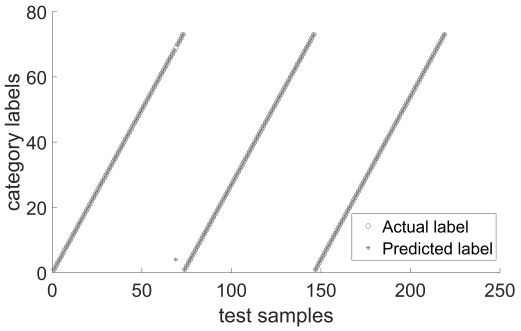

FIGURE 7. Identification result of testing sample.

and sparse representation-SVM. In the wavelet packet transform, the number of decomposition layers is 3 and the wavelet base function is db5. In the PCA, the cumulative principal component contribution rate is $\eta = 90\%$. In the BPNN, the hidden layer function is logsig, the output layer function is tansig, the training function is trainlm, and the mean squared error (MSE) is 0.005. In the K-SVD algorithm, the sparsity is 4, the dictionary size is 30×40, and the number of iterations is 10. The parameters of the different diagnosis methods are shown in Table 3.

TABLE 3. Parameter settings for different methods.

Diagnosis Methods	Parameters
Wavelet Packet−BPNN	INnum=24, MIDnum=32, OUTnum=12, hidden layer function: logsig, output layer function: tansig, MSE=0.005, training function: trainlm
Wavelet Packet−PCA−BPNN	INnum=10, MIDnum=22, OUTnum=12, hidden layer function: logsig, output layer function: tansig, MSE=0.005, training function: trainlm, $\eta = 90\%$
Sparse Representation−BPNN	Sparsity: 4, iterations: 10, dictionary: 30×40, INnum=40, MIDnum=40, OUTnum=12, hidden layer function: logsig, output layer function: tansig, MSE=0.005, training function:trainlm
Sparse Representation−SVM	Sparsity: 4, iterations: 10, dictionary: 30×40, multiclass method: one-against-one, kernel function: RBF

The diagnosis results of different fault diagnosis methods are shown in Table 4. By comparing different methods, we find that the combination of sparse representation and SVM has the highest accuracy in fault diagnosis of NPC three-level inverter. Therefore, the method proposed in this paper is the most advantageous.

TABLE 4. Diagnosis results for different methods.

Diagnosis Methods	Diagnostic Accuracy(%)
Wavelet Packet−BPNN	91.78(201/219)
Wavelet Packet−PCA−BPNN	94.52(207/219)
Sparse Representation− BPNN	98.63(216/219)
Sparse Representation−SVM	99.54(218/219)

VI. CONCLUSION

This paper proposes a combining of sparse representation and SVM for the fault diagnosis of NPC three-level inverter. We first briefly analyzes the circuit structure of NPC three-level inverters and summarizes different fault types. Three-phase phase voltage signals in different fault types are sampled as the characteristic signals. The method of sparse representation is introduced into the fault feature extraction. And the SVM method is used for fault identification. We analyze the influence of K-SVD algorithm parameters on reconstruction error and get a good fault diagnosis result by reasonable parameters setting. Simulation experiments show that the method used in this paper has good diagnostic capability, and the diagnostic accuracy rate is 99.54%.

This paper combines sparse representation and SVM, which are respectively used for fault feature extraction and fault identification. The combination of the two methods can overcome the shortcomings of a single method and better solve the problem of fault diagnosis.

The method of sparse representation is not common for inverter fault feature extraction. In this paper, we have made a preliminary attempt to introduce the signal sparse representation into the fault diagnosis of three-level inverters. Compared with the traditional wavelet transform or PCA, the fault feature information extracted by sparse representation method is easier to identify and the fault diagnosis accuracy rate is higher. Therefore the sparse representation method provides a new idea for fault diagnosis of inverter.

REFERENCES

[1] N. Kumar, T. K. Saha, and J. Dey, "Modeling, control and analysis of cascaded inverter based grid-connected photovoltaic system," *Int. J. Elect. Power Energy Syst.*, vol. 78, pp. 165–173, Jun. 2015.

[2] U.-M. Choi, J.-S. Lee, F. Blaabjerg, and K.-B. Lee, "Open-circuit fault diagnosis and fault-tolerant control for a grid-connected NPC inverter," *IEEE Trans. Power Electron.*, vol. 31, no. 10, pp. 7234–7247, Oct. 2016.

[3] M. B. Abadi, A. M. S. Mendes, and S. M. Â. Cruz, "Method to diagnose open-circuit faults in active power switches and clamp-diodes of three-level neutral-point clamped inverters," *IET Electr. Power Appl.*, vol. 10, no. 7, pp. 623–632, Aug. 2016.

[4] U.-M. Choi, H.-G. Jeong, K.-B. Lee, and F. Blaabjerg, "Method for detecting an open-switch fault in a grid-connected NPC inverter system," *IEEE Trans. Power Electron.*, vol. 27, no. 6, pp. 2726–2739, Jun. 2012.

[5] Y. Wu, Y. Wang, Y. Jiang, and Q. Sun, "Multiple parametric faults diagnosis for power electronic circuits based on hybrid bond graph and genetic algorithm," *Measurement*, vol. 92, pp. 365–381, Oct. 2016.

[6] L. M. A. Caseiro and A. M. S. Mendes, "Real-time IGBT open-circuit fault diagnosis in three-level neutral-point-clamped voltage-source rectifiers based on instant voltage error," *IEEE Trans. Ind. Electron.*, vol. 62, no. 3, pp. 1669–1678, Mar. 2015.

[7] T. Wang, H. Xu, J. Han, E. Elbouchikhi, and M. E. H. Benbouzid, "Cascaded H-bridge multilevel inverter system fault diagnosis using a PCA and multiclass relevance vector machine approach," *IEEE Trans. Power Electron.*, vol. 30, no. 12, pp. 7006–7018, Dec. 2015.

[8] S.-M. Jung, J.-S. Park, H.-W. Kim, K.-Y. Cho, and M.-J. Youn, "An MRAS-based diagnosis of open-circuit fault in PWM voltage-source inverters for PM synchronous motor drive systems," *IEEE Trans. Power Electron.*, vol. 28, no. 5, pp. 2514–2526, May 2013.

[9] T. Wang, J. Qi, H. Xu, Y. Wang, L. Liu, and D. Gao, "Fault diagnosis method based on FFT-RPCA-SVM for cascaded-multilevel inverter," *ISA Trans.*, vol. 60, pp. 156–163, Jan. 2016.

[10] B. Cai, Y. Zhao, H. Liu, and M. Xie, "A data-driven fault diagnosis methodology in three-phase inverters for PMSM drive systems," *IEEE Trans. Power Electron.*, vol. 32, no. 7, pp. 5590–5600, Jul. 2017.

[11] J. Chen *et al.*, "Wavelet transform based on inner product in fault diagnosis of rotating machinery: A review," *Mech. Syst. Signal Process.*, vols. 70–71, pp. 1–35, Mar. 2016.
[12] P. Konar and P. Chattopadhyay, "Multi-class fault diagnosis of induction motor using Hilbert and wavelet transform," *Appl. Soft Comput.*, vol. 30, pp. 341–352, May 2015.
[13] S. Lu, B. T. Phung, and D. Zhang, "A comprehensive review on DC arc faults and their diagnosis methods in photovoltaic systems," *Renew. Sustain. Energy Rev.*, vol. 89, pp. 88–98, Jun. 2018.
[14] F. Wu, Y. Hao, J. Zhao, and Y. Liu, "Current similarity based open-circuit fault diagnosis for induction motor drives with discrete wavelet transform," *Microelectron. Rel.*, vol. 75, pp. 309–316, Aug. 2017.
[15] T. Guo and Z. Deng, "An improved EMD method based on the multi-objective optimization and its application to fault feature extraction of rolling bearing," *Appl. Acoust.*, vol. 127, pp. 46–62, Dec. 2017.
[16] D. Y. Jung, S. M. Lee, H.-M. Wang, J. H. Kim, and S. H. Lee, "Fault detection method with PCA and LDA and its application to induction motor," *J. Central South Univ. Technol.*, vol. 17, no. 6, pp. 1238–1242, 2010.
[17] L. I. Kuncheva and W. J. Faithfull, "PCA feature extraction for change detection in multidimensional unlabeled data," *IEEE Trans. Neural Netw. Learn. Syst.*, vol. 25, no. 1, pp. 69–80, Jan. 2014.
[18] C. Ma, X. Gu, and Y. Wang, "Fault diagnosis of power electronic system based on fault gradation and neural network group," *Neurocomputing*, vol. 72, nos. 13–15, pp. 2909–2914, 2009.
[19] R. B. Dhumale and S. D. Lokhande, "Neural network fault diagnosis of voltage source inverter under variable load conditions at different frequencies," *Measurement*, vol. 91, pp. 565–575, Sep. 2016.
[20] D. Chen and Y. Ye, "Fault diagnosis of three level inverter based on multi neural network," *Trans. China Electrotech. Soc.*, vol. 28, no. 6, pp. 120–126, 2013.
[21] Y.-K. Liu, F. Xie, C.-L. Xie, M.-J. Peng, G.-H. Wu, and H. Xia, "Prediction of time series of NPP operating parameters using dynamic model based on BP neural network," *Ann. Nucl. Energy*, vol. 85, pp. 566–575, Nov. 2015.
[22] H. Tang, J. Chen, and G. Dong, "Sparse representation based latent components analysis for machinery weak fault detection," *Mech. Syst. Signal Process.*, vol. 46, no. 2, pp. 373–388, 2014.
[23] Z. Feng, Y. Zhou, M. J. Zuo, F. Chu, and X. Chen, "Atomic decomposition and sparse representation for complex signal analysis in machinery fault diagnosis: A review with examples," *Measurement*, vol. 103, pp. 106–132, Jun. 2017.
[24] X. Ding and Q. He, "Time–frequency manifold sparse reconstruction: A novel method for bearing fault feature extraction," *Mech. Syst. Signal Process.*, vol. 80, pp. 392–413, Dec. 2016.
[25] Z. Feng and M. Liang, "Complex signal analysis for planetary gearbox fault diagnosis via shift invariant dictionary learning," *Measurement*, vol. 90, pp. 382–395, Aug. 2016.
[26] G. He, K. Ding, and H. Lin, "Fault feature extraction of rolling element bearings using sparse representation," *J. Sound Vibrat.*, vol. 366, pp. 514–527, Mar. 2016.
[27] Q. He and X. Ding, "Sparse representation based on local time–frequency template matching for bearing transient fault feature extraction," *J. Sound Vib.*, vol. 370, pp. 424–443, May 2016.
[28] H. Liu and S. Li, "Target detection using sparse representation with element and construction combination feature," *IEEE Trans. Instrum. Meas.*, vol. 64, no. 2, pp. 290–298, Feb. 2015.
[29] H. Li, F.-L. Chung, and S. Wang, "A SVM based classification method for homogeneous data," *Appl. Soft Comput.*, vol. 36, pp. 228–235, Nov. 2015.
[30] C. Jing and J. Hou, "SVM and PCA based fault classification approaches for complicated industrial process," *Neurocomputing*, vol. 167, pp. 636–642, Nov. 2015.
[31] R. Wang, Y. Zhan, H. Zhou, and B. Cui, "A fault diagnosis method for three-phase rectifiers," *Int. J. Elect. Power Energy Syst.*, vol. 52, pp. 266–269, Nov. 2013.
[32] I. Abari, A. Lahouar, M. Hamouda, J. B. H. Slama, and K. Al-Haddad, "Fault detection methods for three-level NPC inverter based on DC-bus electromagnetic signatures," *IEEE Trans. Ind. Electron.*, vol. 65, no. 7, pp. 5224–5236, Jul. 2018.
[33] M. Aharon, M. Elad, and A. Bruckstein, "*K*-SVD: An algorithm for designing overcomplete dictionaries for sparse representation," *IEEE Trans. Signal Process.*, vol. 54, no. 11, pp. 4311–4322, Nov. 2006.
[34] C. Rusu and B. Dumitrescu, "Stagewise K-SVD to design efficient dictionaries for sparse representations," *IEEE Signal Process. Lett.*, vol. 19, no. 10, pp. 631–634, Oct. 2012.
[35] S. S. Chen, D. L. Donoho, and M. A. Saunders, "Atomic decomposition by basis pursuit," *SIAM Rev.*, vol. 43, no. 1, pp. 129–159, 2001.
[36] S. Narayanan, S. K. Sahoo, and A. Makur, "Greedy pursuits assisted basis pursuit for reconstruction of joint-sparse signals," *Signal Process.*, vol. 142, pp. 485–491, Jan. 2018.
[37] S. G. Mallat and Z. Zhang, "Matching pursuits with time-frequency dictionaries," *IEEE Trans. Signal Process.*, vol. 41, no. 12, pp. 3397–3415, Dec. 1993.
[38] S. E. Ferrando, E. J. Doolittle, A. J. Bernal, and L. J. Bernal, "Probabilistic matching pursuit with Gabor dictionaries," *Signal Process.*, vol. 80, no. 10, pp. 2099–2120, 2000.
[39] J. A. Tropp and A. C. Gilbert, "Signal recovery from random measurements via orthogonal matching pursuit," *IEEE Trans. Inf. Theory*, vol. 53, no. 12, pp. 4655–4666, Dec. 2007.
[40] V. Vapnik, *The Nature of Statistical Learning Theory*. York, U.K.: Springer-Verlag, 2000.
[41] Z. Yin and J. Hou, "Recent advances on SVM based fault diagnosis and process monitoring in complicated industrial processes," *Neurocomputing*, vol. 174, pp. 643–650, Jan. 2016.
[42] Z. Li *et al.*, "Online implementation of SVM based fault diagnosis strategy for PEMFC systems," *Appl. Energy*, vol. 164, pp. 284–293, Feb. 2016.
[43] H. Guo and W. Wang, "An active learning-based SVM multi-class classification model," *Pattern Recognit.*, vol. 48, no. 5, pp. 1577–1597, 2015.
[44] D. J. Bordoloi and R. Tiwari, "Optimum multi-fault classification of gears with integration of evolutionary and SVM algorithms," *Mechanism Mach. Theory*, vol. 73, pp. 49–60, 2014.
[45] B. Liu, Y. Xiao, and L. Cao, "SVM-based multi-state-mapping approach for multi-class classification," *Knowl.-Based Syst.*, vol. 129, pp. 79–96, Aug. 2017.

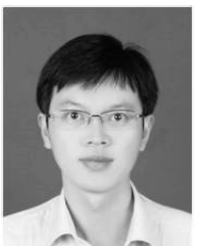

YUNJUN YU was born in Shangrao, China. He received the B.Sc. degree in automation and the M.Sc. degree in control theory and control engineering from Nanchang University in 2000 and 2007, respectively, and the Ph.D. degree from the Chinese Academy of Sciences in 2013. He is currently an Associate Professor with the Department of Electrical and Automation Engineering, Information Engineering School, Nanchang University, China. His research interests include fault diagnosis, data-driven optimal control and it's applied in photovoltaic micro-grid systems, ADRC, and low-carbon electricity technology.

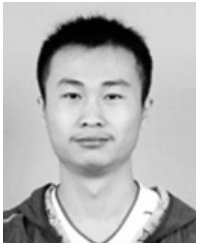

SHILEI PEI received the B.S. degree in biomedical engineering from Zhengzhou University, Henan, China, in 2015, where he is currently pursuing the M.S. degree in control science and engineering with Nanchang University, Jiangxi, China.

His research interest mainly focuses on inverter fault diagnosis.